Inverse modelling of the ETEX-1 release with a Lagrangian particle model

Petra Seibert*
Institute of Meteorology and Physics
University of Agricultural Sciences
Türkenschanzstr. 18, A-1180 Vienna, Austria
seibert@boku.ac.at, http://boku.ac.at/imp/envmet/

Andreas Stohl
Lehrstuhl für Bioklimatologie und Immissionsforschung,
Technical University of Munich, Freising, Germany
http://www.fw.tum.de/LST/METEOR/stohl/astohl.html

Abstract

The derivation of source-receptor matrices for a passive, nonreacting and nondepositing tracer from backward runs of a Lagrangian particle dispersion model is shown. This technique is applied to the first release of the European Tracer Experiment ETEX. The source-receptor matrix is used to invert measurements to obtain the temporal evolution of the release with given release location as a first illustration and test of the method.

1 Introduction

The purpose of this study was to test the potential of inverse modelling with data from the European Tracer Experiment ETEX [2, 3]. In this context, inverse modelling means to derive information on a source of an atmospheric trace constituent from ambient concentration measurements, using a dispersion model for the description of the source-receptor relationship. At first, we show how a Lagrangian particle dispersion model (LPDM) can

*This work is a contribution to EUROTRAC-2 subprojects GLOREAM and GENEMIS-2, funded by FWF under P1295-GEO. Meteorological data from ECMWF have kindly been provided through ZAMG (Vienna).

be used in a backward mode to derive source-receptor matrices. This is a novel approach. Then the technique is applied to the ETEX release and a regularised inversion is performed to deduct the temporal evolution of the release. This is, however, just a very first application, and the outlook outlines possible refinements and further evaluations.

There are a number of different approaches to inverse modelling of atmospheric trace constituents. For a linear problem (ambient concentrations proportional to the source strength), one can obtain the unknown source from the solution of a linear system of equations, with measurements as knowns and elements of the source-receptor matrix (SRM) as coefficients. Depending on the number of knowns and unknowns as well as the conditioning of the matrix, one often needs to apply a so-called regularisation (input of a-priori knowledge) [6]. The SRM can be obtained by forward or backward modelling, and with a Lagrangian or a Eulerian model. The backward approach is most efficient when the number of unknown source elements exceeds the number of measurements. Lagrangian models have the advantage compared to Eulerian models that they have a better numerical accuracy (mainly, no numerical diffusion due to the advection scheme), and that they do not suffer from a grid resolution problem near point sources. In the backward mode, this is especially important because measurements are almost always made at a point or along a line (aircraft) and with Eulerian models one would need to apply a near-source sub-model or else loose once more in accuracy.

The other approach is to search iteratively for the minimum of a cost function, made up by the misfit between measurements and model, and a regularisation term if necessary. This requires the calculation of the gradient of this cost function with respect to the source elements. Often, this approach is realised with a Eulerian model and its adjoint, the only viable approach for large nonlinear problems [1]. It is also possible to use a Eulerian model and its adjoint for the determination of a SRM by defining suitable cost functions.

2 Derivation of the source-receptor matrix

2.1 Forward and backward simulations with a LPDM

In the forward mode, particles are released from prescribed source areas, and transported with the mean and turbulent velocity field. They carry a mass depending on source strength and particle release rate. It can be altered by processes such as deposition or decay. Concentrations are calculated by summing up the masses of all the particles in a grid cell, and dividing the sum by the cell's volume.

In the backward mode, used for inverse modelling, the same formalism and computer model are applied, but the particle trajectories are integrated backward in time, using a negative time step. However, there is a new interpretation: particle masses are replaced by mixing ratios $\chi \equiv c/\rho$ (where c is the mass concentration and ρ the air density) in an infinitesimal volume of air. In our Lagrangian frame of reference, χ can change only by sinks such as deposition or decay and by uptake of emissions. Without deposition, the individual rate of change of the mixing ratio is

$$\frac{d\chi}{dt} = S_\chi, \tag{1}$$

where S_χ denotes the alteration of χ by sources S^+ and sinks S^-.

The sources are independent of χ, and sinks not considered as we are dealing with an inert tracer[1]. Eq. 1 can be easily integrated, yielding the instantaneous concentration. In ETEX (and many other practical applications), measured concentrations represent a point in space and an average in time (ETEX: sampling interval 3 h). Thus, we need to average in time. If this averaging time exceeds substantially the time scale of the turbulent fluctuations, the temporal averaging alone is sufficient and additional ensemble averaging is not necessary. Next, we introduce a discretisation in time (index j) with J back trajectories in equal intervals between t_1 and t_2, and index i for the temporal and spatial variation of S^+ ("gridded in space and time"):

$$\overline{\chi} \equiv \frac{1}{t_2 - t_1} \int_{t_1}^{t_2} \chi(\boldsymbol{x}, t)dt \approx \sum_i \left[S_i^+ \left(\frac{1}{J} \sum_j \Delta t'_{ij}\right) \right]. \tag{2}$$

The term in parenthesis on the right-hand side is equal to $\Delta\tau_i$, the average residence time of all J trajectories in a spatio-temporal cell i contributing to the measurement under consideration.

Let us now consider that we have not just one measurement, but many (different sites and times), denoted by l. Then we see that the elements of

[1]The following derivation is restricted to the case without sinks. However, it is intuitively clear that the LPDM can be applied in the same way also for the linear case with sinks, as the relative magnitude of any loss along a certain transport distance is the same in the forward and in the backward mode. The exact derivation will be presented later.

the desired source-receptor matrix $\boldsymbol{M}$ are

$$M_{il} \equiv \frac{\partial \overline{\chi}_l}{\partial S_i^+} = \Delta\tau_{il}. \tag{3}$$

If we call the vectors of observations ($\overline{\chi}_l$) and emissions (S_i^+) $\boldsymbol{y}$ and $\boldsymbol{x}$, respectively, we arrive at the linear system of equations (LSE) to be solved for the inverse modelling:

$$\boldsymbol{y} = \boldsymbol{M}\boldsymbol{x}. \tag{4}$$

If the density variations between the receptors and the sources are small, mixing ratios χ may be substituted by mass concentrations, and S^+ by the emitted mass per volume and time, the parameter used normally. Otherwise, χ and S^+ can be transformed with the air density (climatological values are sufficient).

2.2 Implementation in the Lagrangian particle model FLEXPART

The Lagrangian particle dispersion model FLEXPART (details see section 3.2) was used in this application. FLEXPART gives gridded concentration fields as output. How can we obtain gridded residence times from this output? The time-averaged concentration in a grid cell $\bar{c}_i$ as computed in FLEXPART can be written as

$$\bar{c}_i = \frac{\mu_{tot}}{V_i\ NJ} \sum_{n=1}^{N}\sum_{j=1}^{J} f_{ijn}, \tag{5}$$

where V_i is volume of the grid cell, N the number of instants in time used to form a temporal average over an interval ΔT, μ_{tot} the total released mass, and f_{ijn} the fraction of the mass of a particle attributed to a specific grid cell, considering that all J particles have the same mass because there are no sinks.

Using the residence fraction f, the average residence time $\Delta\tau_i$ during ΔT can be calculated as

$$\Delta\tau_i = \frac{\Delta T}{NJ} \sum_{n=1}^{N}\sum_{j=1}^{J} f_{ijn}. \tag{6}$$

Combining (5) and (6), we obtain

$$\Delta\tau_i = \bar{c}_i \, \frac{V_i \, \Delta T}{\mu_{tot}}. \tag{7}$$

This means that the desired residence times can be obtained by a backward run of the regular FLEXPART model, transforming the resultant concentrations according to (7). The spatial and temporal resolution of the sources is given by the V_i and ΔT used in the concentration calculation of FLEXPART.

3 ETEX application

3.1 Key features

The European Tracer Experiment ETEX comprised two releases of a gaseous, nondepositing, inert tracer. We are dealing here only with the first one. This experiment can be characterised as follows [2, 3]:

- Release location: Bretagne (NW France)
- Release time: 23 Oct 16:00 UTC – 24 Oct 3:50 UTC, 1994 (11:50 h duration)
- Release rate: 7.98 g/s (constant)
- Sampling network: 168 stations over most of western and central Europe
- Sampling resolution: 3 hours
- Sampling duration: 30 intervals (90 h)

In the context of backward modelling, confusion can easily arise because, for example, the physical receptors are used as sources in the inverse model runs, whereas the physical source location acts as a receptor location. Therefore, we introduce the following notation: *Source*, *concentration*, *receptor*, etc. denote the physical system or a forward simulation; the same words with a * refer to the backward simulation. Thus, for example, a *receptor* is used as a *source**.

3.2 FLEXPART setup for the inverse model run

FLEXPART is a LPDM developed by Andreas Stohl, and tested on various tracer experiments [8]. It performed well for the ETEX-1 release (correlation coefficient between observations and simulated concentrations 0.59, fractional bias 0.01).

FLEXPART was run with the following specifications:

- Input: ECMWF fields (1.0°, 31 levels as spatial and 3 h as temporal resolution).
- 30 backward runs (one for each sampling interval)
- 10,000 particles released from each monitoring site
- each monitoring site (release* location) is one species
- output sampled with 3 h intervals on a 41×21 grid with 1° resolution, 9 vertical cells (0/75/150/300/600/1200/2400/3600/4800/6000 m), 35 time intervals

Thus, the size of our source-receptor matrix is $(41\times21\times9\times35) \times (168\times30) = 180{,}810 \times 5{,}740 \approx 1.4 \cdot 10^9$ elements. In sparse matrix format, this amounts to $\approx$ 300 MByte of data. This matrix is too big for direct evaluation. Therefore, we have to consider the following options for simplifications:

1) Take only the lowest layer (or a vertical integral) as potential source, as concentrations* were well mixed near the release site.

2) Assume either the location as given (sample application: nuclear power plant accident), or release time (sample application: nuclear explosion with explosion time known from nuclide ratios).

3) Start with a coarse source resolution and narrow it down iteratively while reducing the domain size, horizontally, vertically, and/or temporally.

Here, we have applied simplifications 1 and 2 (release location given).

3.3 First visualisation of results

For a first visualisation, we plot fields that would result if a backward simulation would have been made with releases* proportional to the measured concentrations at each receptor. The plot may show horizontal fields for one time interval (or a loop over the whole simulation), a time-height-section at the release site, or just the time evolution at the release site. All these evaluations can be done for each monitoring site separately, or as the sum of all of them. This corresponds to classical "trajectory statistics" [7], or the "adjoint tracer" fields presented by Pudykiewicz [4]. This is not yet an inversion, but it is nice to illustrate the backward simulation.

Figure 1 shows that this method gives already a good picture of the timing of the release. The maximum lies within the real release interval for most stations, but some of them (e.g., D30 = Mannheim in Germany) are clear outliers. Figure 2 gives an idea how the "adjoint tracer" cloud* looks like at different times. The left frame is at the time of the release and shows its maximum near the release location while the right frame is

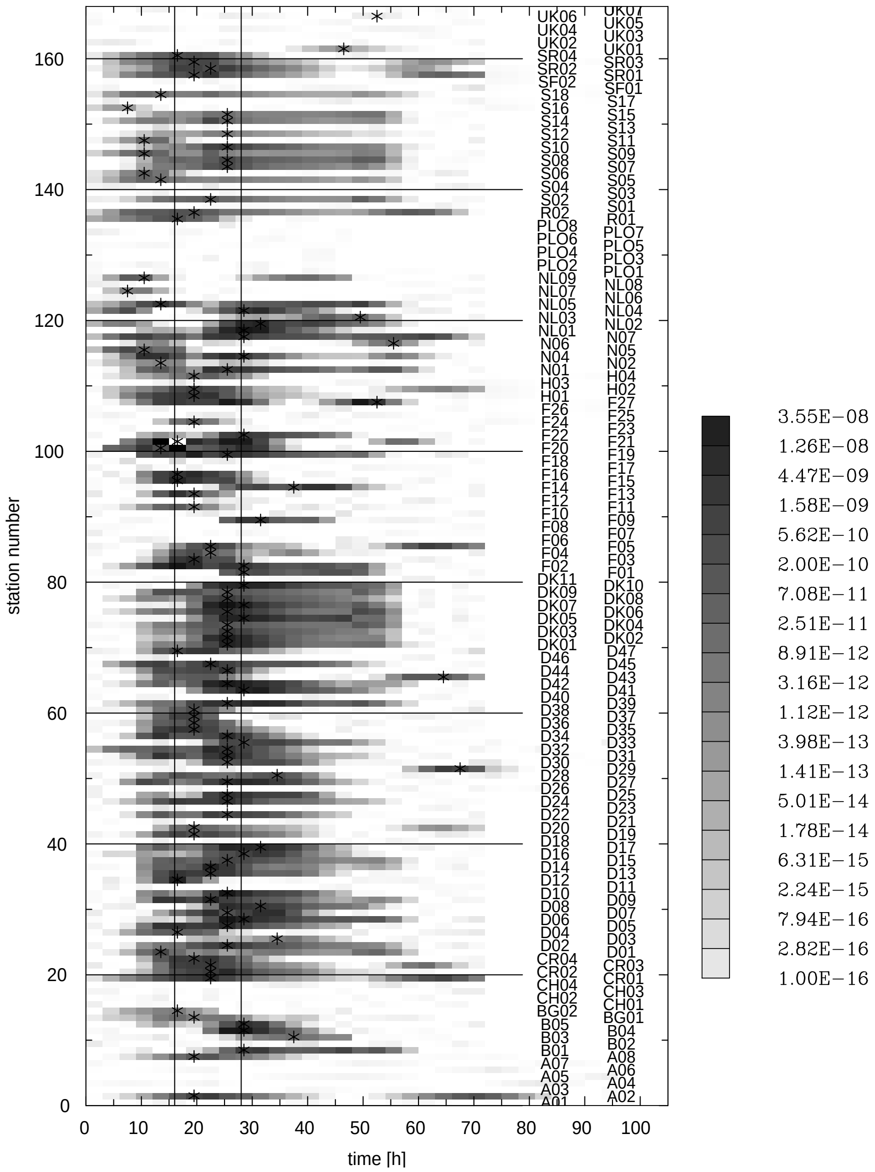

Figure 1: Time series of a tracer* released at the measurements sites proportional to measured tracer concentrations, sampled at the true release site. Each line corresponds to one measurement location (denoted by its ETEX station code) and the sum over all measurement intervals. Asterisks denote the maxima, and vertical lines the begin and end of the release. Note the logarithmic scale.

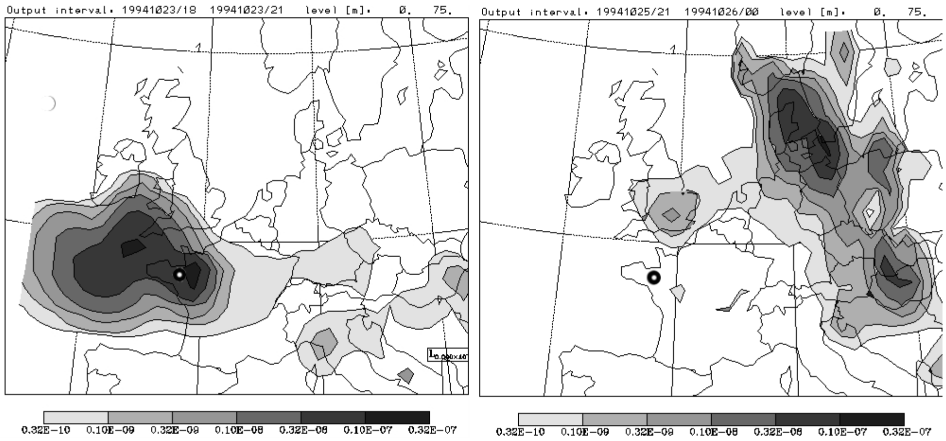

Figure 2: Horizontal distribution of a tracer* released at the measurements sites proportional to measured tracer concentrations. Note the logarithmic scale. The real release location is marked by a hollow black dot. The left panel shows the tracer during the time of the real release (23 Oct, 18-21 UTC), the right panel at a previous stage of the inverse simulation (25 Oct, 21-24 UTC).

at a later time (previos stage of the backward simulation) and looks similar to the "real" cloud at this stage as depicted by measurements. This figure may be compared with Fig. 3 in [5].

3.4 Inversion of temporal release evolution

We perform a generalised inversion (this means a regularised solution, see [6]) of the LSE $\boldsymbol{y^o} \approx \boldsymbol{Mx}$ (Eq. 4), where $\boldsymbol{y^o}$ are the observations, minimising the cost function

$$J = ||\boldsymbol{y^o} - \boldsymbol{M}\hat{\boldsymbol{x}}||^2 + \theta^2 ||\hat{\boldsymbol{x}}||^2 \tag{8}$$

in order to obtain the source $\boldsymbol{x}$ as a function of time, assuming the location as given. The source-receptor matrix for the release point is obtained by linear interpolation from the four surrounding cells. All data are used, and the full time range between 23 Oct 12 UTC and 27 Oct 12 UTC is used, in contrast to [5].

Figure 3 shows the result. We see that the start of the release was accurately captured. The end of the release was found well but is too fuzzy and slightly biased towards later times. As the peak caused by station

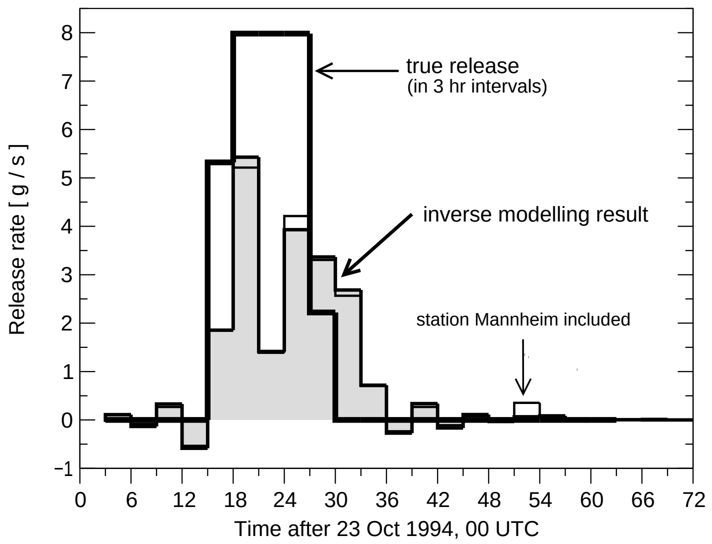

Figure 3: ETEX Release 1, true time-dependent release rate (merged into 3 h intervals) and release rate obtained by inverse modelling (with and without the outlier station Mannheim).

Mannheim at 50 h shows, the inversion is disturbed to some extent by outliers.

Observed concentrations and concentrations computed by following methods have been compared as a test.

- FWD: Forward simulation made by A. Stohl [8] with true source term $\boldsymbol{x_t}$
- BWD-i1: Concentrations obtained as $\boldsymbol{M}\hat{\boldsymbol{x}}$ where $\hat{\boldsymbol{x}}$ denotes the source term estimated by inverse modelling
- BWD-i2: Concentrations obtained as $\boldsymbol{M}\hat{\boldsymbol{x}}^*$ where $\hat{\boldsymbol{x}}^* = \hat{\boldsymbol{x}}\ |\boldsymbol{x_t}|\ /\ |\hat{\boldsymbol{x}}|$ (scaled source term)
- BWD-t: Concentrations obtained as $\boldsymbol{M}\boldsymbol{x_t}$ (true source term, transformed to 3 h resolution)

The results are presented in Table 1. We see that the SRM of the inverse run yields worse results than the forward run, but results with the reconstructed source term are better than with the real source term with respect to correlation and RMS error (not, of course, for bias). The total release is underestimated by 35% inspite of an unbiased forward simulation.

We can thus conclude that the backward simulation suffers from the 3-hourly temporal and the grid-cell horizontal resolution of the source. The bias is obviously caused by formulation of cost function in combination with simulation errors.

Table 1: Statistical performance indicators for the comparison modelled – measured tracer concentrations. Meaning of abbreviations for the method see text.

Method	r	relative bias	relative RMSE	$\lvert\boldsymbol{x}\rvert$
FWD	0.59	≈ 0.01	?(not published)	340 kg
BWD-i1	0.44	–0.35	1.84	208 kg
BWD-i2	0.44	+0.05	2.99	340 kg
BWD-t	0.33	+0.13	3.51	340 kg

4 Conclusions and outlook

Backward simulations with a LPDM have successfully been established as a tool for the generation of source-receptor matrices. This method is attractive with respect to accuracy and computational effort. It yields useful results already in this first implementation, and it can be expected that it will improve after the following steps:

- Test the effect of better temporal resolution of the source.
- Introduce weighting of observations according to the error associated with them, to reduce the influence of outliers.
- Do inverse modelling for finding the source location and the joint time-space location.
- Test more sophisticated regularisation methods.

In the future, this method shall be applied also to other tracer experiments such as ANATEX and CAPTEX as well as to the release from the Chernobyl NPP disaster. Finally, the method may be used for unknown sources.

References

[1] Elbern H., and H. Schmidt, *A four-dimensional variational chemistry data assimilation scheme for Eulerian chemistry transport modeling.* J. Geophys. Res. **104**(D15) (1999), 18,583-18589.

[2] *ETEX, a European tracer experiment*, Atmos. Environ. **32**, Vol. 24 (special issue) (1998).

[3] *ETEX. The European tracer experiment*, European Communities, Publ. No. EUR 18143EN, ISBN 92-828-5007-2, 107 pp., 1998.

[4] Pudykiewicz J. A., *Application of adjoint tracer transport equations for evaluating source parameters.* Atmos. Environ. **32** (1998), 3039-3050.

[5] Robertson L., and J. Langner, *Source function estimate by means of a variational data assimilation applied to the ETEX-I tracer experiment.* Atmos. Environ. **32**(24) (1998), 4219-4225.

[6] Seibert P., *Inverse modelling of sulfur emissions in Europe based on trajectories*, Inverse Methods in Global Biogeochemical Cycles, AGU Geophysical Monograph Vol. 114, 1999, pp. 147-154.

[7] Stohl A., *Computation, accuracy and applications of trajectories – a review and bibliography.* Atmos. Environ. **32** (1998), 947-966.

[8] Stohl A., M. Hittenberger, G. Wotawa, *Validation of the Lagrangian particle dispersion model FLEXPART against large scale tracer experiments*, Atmos. Environ. **32**(24) (1998), 4245-4264.